RSC Advances

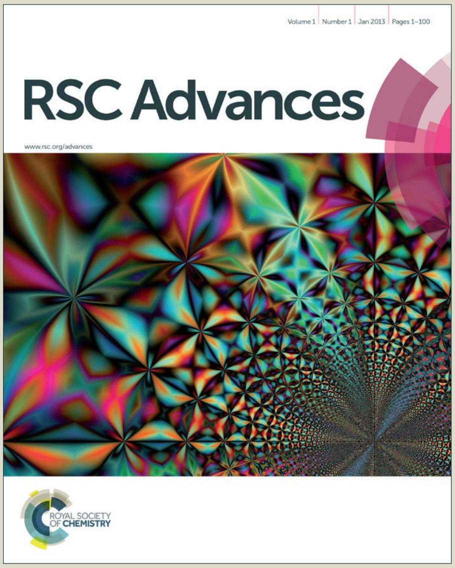

ROYAL SOCIETY OF CHEMISTRY

www.rsc.org/advances

RSC Advances

PAPER

Synthesis and Characterization of Protic Ionic Liquids as Thermoelectrochemical Materials

Received 00th January 20xx,
Accepted 00th January 20xx

DOI: 10.1039/x0xx00000x
www.rsc.org/

T. A. Siddique,[a] S. Balamurugan,[a] S. M. Said,[a,*] N. A. Sairi,[b] and W. M. D. W. Normazlan[b]

Abstract

Unique work report on the thermoelectrochemical potential of protic ionic liquid (PIL) based electrolytes coupled with I^-/I_3^- redox couple. Two series of protic ionic liquids based on secondary and/or tertiary ammonium cations with the trifluoroacetate, methanesulfonate, trifluoromethanesulfonate and tosylate anions were synthesized for thermoelectrochemical cells. The complete study on PILs was carried out to determine the nature and efficiency for the generation of voltage through electrochemical effect. The investigation was executed in a temperature range between room temperature and 90 °C. PILs show lower thermal conductivity and good ionic conductivity which leads to the success of good thermoelectric materials. The outcome was positive as our proposed PILs showed higher S_e values 420 μV/K obtained for TEHA TFMS than the reported values of the same I^-/I_3^- redox couple. The most favorable thermoelectric figure of merit value (949.46×10^{-6}) was achieved by the BEHA TFMS. The power and the current output of the studied PILs are higher than some aprotic ionic liquids (AILs) reported.

Keywords: Ammonium based protic ionic liquids, secondary and tertiary ammonium, thermal properties, physical properties, iodide/tri-iodide (I^-/I^{3-}) redox couple, ionic and thermal conductivity, Seebeck Coefficient, ZT, power and current output.

Introduction

Renewable energy resources are a current global concern, given the depletion of fossil fuels, along, with the detrimental effects of fossil fuel burning such as global warming and environmental pollution. Over 50% of energy is lost as waste heat during the fossil fuel burning process for energy generation. While the dependence on fossil fuels cannot be fully overcome, thermoelectric technology provides a secondary energy generation technology which can be used in tandem with fuel engines, in order to harvest the waste heat into useful electricity.[1, 2]

Several classes of materials have been utilised as thermoelectric materials: inorganic semiconductor alloys such as bismuth telluride and lead in terms of performance and commercialisation development. However, such alloys have drawbacks such as high synthesis and fabrication costs, complex manufacturing processes and limited natural resources. In recent years, organic thermoelectric materials have been shown to be viable candidates for thermoelectric generation, such as PEDOT:PSS. Even more recently, Ionic liquids (ILs) doped with a redox couple have been shown to demonstrate an electrochemically driven thermoelectric generation capability, which is also known as the thermoelectrochemical effect.[3-7] These IL based devices differ in operation from the semiconductor based thermoelectrics, as they are driven by a redox electrochemical reaction which arises from a temperature gradients. Thermoelectric devices are prepared from thermoelectric cells, which are an array of thermoelectrochemical cells electrically connected in series but thermally in parallel. As reviewed by MacFarlane *et al.*,[8] the thermoelectrochemical cells may directly convert thermal energy into electrical energy,[9, 10] which limits their operating temperature to less than 100 °C.

ILs are organic salts with melting points generally below 100 °C and structured in three dimensional networks of ions (anions and cations). These ILs may be divided into two main categories, which are protic ionic liquids (PILs) and aprotic ionic liquids (AILs).[11] PILs are synthesized by a proton transfer between a stoichiometric Brønsted acid to a Brønsted base.[12] Some groups reported on their study of thermoelectrochemical cells development using AILs[3-5, 7] and PILs[6] as electrolytes to generate electrical energy. The PILs are advantageous for the development of thermoelectrochemical devices, because it implies that only moderate solubilities are required for the most efficient devices.

The first discovered IL, ethanolammonium nitrate (EAN) which has been reported by Gabriel in 1888,[13] was later

---

[a] Electrical Engineering Department, Faculty of Engineering, University of Malaya, 50603 Kuala Lumpur, MALAYSIA. E-mail: smsaid@um.edu.my, cheksu@gmail.com, tawsif.mme07@gmail.com
[b] Chemistry Department, Faculty of Science, University of Malaya, 50603 Kuala Lumpur, MALAYSIA

†Electronic Supplementary Information (ESI) available: [^{1}H-NMR graps and tabulated data of physical and electrochemical properties]. See DOI: 10.1039/x0xx00000x

proven to be a PIL by Walden in 1914.[14] EAN was prepared by a proton transfer reaction from a Brønsted acid and a Brønsted base without using any solvents, with 12.5 °C as the melting temperature.[15] The main difference between PILs and AILs is the presence of an available proton in PILs which is responsible for the extra hydrogen bonding. Thus, PILs may comprise of neutral species which are produced by proton transfer equilibrium processes and hence, do not necessarily contain fully ionic components. In 2007, MacFarlane and Seddon have proposed a guideline for determining “pure ILs”, where it is necessary that the presence of neutral species should be less than 1 %.[16]

Recently, there is an increasing interest towards PILs, as well as greater attention to AILs.[11] This is owing to its special property in the presence of proton-donor and -acceptor sites as it may be used to build up a hydrogen-bonding network. As an addition, the preparation of PILs is simple, as both, the synthesis and purification processes are easy, less expensive, have low toxicity and degradable.[17-19] Due to their beneficial properties and potential applications, PILs are now used for fuel cells,[11] organic synthesis,[20] gas separation,[21] biological applications,[22] chromatography,[15] CO_2 absorption,[23] self-assembly,[24] as electrolyte in batteries,[24] conductors,[25] as propellant or explosives,[26] as catalysts in chemical reactions,[27] as solvents of rare polymers[28, 29] and as reactants in biodiesel production.[30]

Knowledge of thermal and physicochemical properties are important to determine the potential applications of the synthesized PILs. Recently, researchers have been discussing these thermal properties including heat capacity, phase transition temperatures and decomposition temperatures; as well as physicochemical properties such as density, viscosity, speed of sound, refractive index and ionic conductivity in some recent publications.[17, 18, 31-36] In these reports, most cases were investigated on a series of PILs with alkyl ammonium, hydroxyl ammonium or hydroxylalkyl ammonium –based cations and carboxylate-based anions.

In this study, two series of ammonium-based PILs have been synthesized. The aim of this study is to evaluate significant fundamental data on thermal, physicochemical and thermoelectric properties of the BEHA and TEHA series for their potential application as thermoelectric materials. The thermal properties such as the decomposition temperature, melting temperature, heat of fusion and heat capacity of studied PILs have been analysed. The physicochemical properties such as density, viscosity and refractive index have also been investigated. Lastly and mainly, we will discuss the thermoelectric properties, namely the ionic and thermal conductivity, the Seebeck coefficient, the figure of merit and the power and current output density of these 8 PILs in combination with the standard aqueous I^-/I_3^- electrolyte system to evaluate the overall potentiality of PILs as thermoelectric materials.

Experimental

Materials and synthesis of PILs

Bis(2-ethylhexyl) amine (99%) and tris(2-ethylhexyl) amine (99 %), trifluoroacetic acid (99%), methanesulfonic acid (99%), trifluoromethanesulfonic acid (99%), ρ-toluenesulfonic acid (99%) were purchased from Merck. These chemicals were used as received without any further purification. PILs are formed by proton transfer between a Brönsted acid and a Brönsted base. An equimolar amount of acid and base will be reacted. The drop wise addition of acids to the amine was carried out slowly with continuous stirring with a magnetic bar, since these reactions are highly exothermic. Hence, a slight amount of water was added to reduce the heat. The mixture was then stirred at room temperature for several hours. Strong agitation was applied in order to improve the contact between the reactants, allowing the reaction to be completed. The reaction is a simple Brönsted acid-base neutralization forming an ionic liquid. Then, water was removed by heating the mixture at 80 °C in vacuum using a rotary evaporator. The PILs were further dried at 80 °C in a vacuum oven to remove any excess water. The fully distilled and dried PILs purity was checked by a ^{1}H NMR spectroscopy.

	Names	Abbreviations
1	Bis(2-ethylhexyl) ammonium Trifluoroacetate	BEHA TFA
2	Bis(2-ethylhexyl) ammonium Methanesulfonate	BEHA MS
3	Bis(2-ethylhexyl) ammonium Trifluoromethanesulfonate	BEHA TFMS
4	Bis(2-ethylhexyl) ammonium Tosylate	BEHA Tosylate
5	Tris(2-ethylhexyl) ammonium Trifluoroacetate	TEHA TFA
6	Tris(2-ethylhexyl) ammonium Methanesulfonate	TEHA MS
7	Tris(2-ethylhexyl) ammonium Trifluoromethanesulfonate	TEHA TFMS
8	Tris(2-ethylhexyl) ammonium Tosylate	TEHA Tosylate

Table 1: Names and Abbreviation of Synthesized PILs

BEHA TFA: ^{1}H NMR (400 MHz, $CDCl_3$, ppm): δ =0.91 (t, J=7.4 Hz, 12H, $-CH_3$), 1.19-1.49 (m, 16H, $-CH_2$), 1.65-1.93 (m, 2H, -CH), 2.57 (d, 4H, J=8.2 Hz, $-CH_2$) and 8.37 (2H, NH & $NH^+CF_3COO^-$).

BEHA MS: ^{1}H NMR (400 MHz, $CDCl_3$, ppm): *δ* =0.82 (t, J=7.3 Hz, 12H, $-CH_3$), 1.19-1.26 (m, 16H, $-CH_2$), 1.70-1.78 (m, 2H, -CH), 2.62 (s, 3H, $-CH_3SO_2^-$), 2.79 (d, 4H, J=8.0 Hz, $-CH_2$), and 8.37 (2H, NH & $NH^+CH_3SO_3^-$).

BEHA TFMS: ^{1}H NMR (400 MHz, $CDCl_3$, ppm): *δ* =0.88 (t, 12H, J=6.9 Hz, $-CH_3$), 1.24-1.39 (m, 16H, $-CH_2$), 1.73-1.75 (m, 2H, -CH), 2.85 (d, 4H, J=8.0 Hz, $-CH_2$) and 6.6 (2H, NH & $NH^+CF_3SO_3^-$).

BEHA Tosylate: ^{1}H NMR (400 MHz, $CDCl_3$, ppm): δ =0.82 (t, 12H, J=7.0 Hz, $-CH_3$), 1.19-1.28 (m, 16H, $-CH_2$), 1.70-1.72 (m, 2H, -CH), 2.34(s, 3H, $-Ar-CH_3$), 2.63 (d, 4H, J=7.2 Hz, $-CH_2$), 7.14 (2H, d, J=4.1 Hz, Ar-H), 7.73 (2H, d, J=4.2 Hz, Ar-H) and 9.37 (2H, NH & NH^+tosylate$^-$).

TEHA TFA: ^{1}H NMR (400 MHz, $CDCl_3$, ppm): δ =0.81 (t, J=5.4 Hz, 18H, $-CH_3$), 1.20-1.35 (m, 24H, $-CH_2$), 2.06-2.08 (m, 3H, -CH), 2.88 (d, 6H, J=10.2 Hz, $-CH_2$) and 11.05 (1H, $NH^+CF_3COO^-$).

TEHA MS: ^{1}H NMR (400 MHz, $CDCl_3$, ppm): δ =0.82 (t, J=6.2 Hz, 18H, $-CH_3$), 1.21-1.34 (m, 24H, $-CH_2$), 1.59-1.60 (m, 3H, -CH), 2.47 (s, 3H, $-CH_3SO_2^-$), 2.96 (d, 6H, J=12.0 Hz, $-CH_2$) and 9.1 (1H, $NH^+CH_3SO_3^-$)

TEHA TFMS: ^{1}H NMR (400 MHz, $CDCl_3$, ppm): δ =0.88 (t, 18H, J=6.8 Hz, $-CH_3$), 1.24-1.48 (m, 24H, $-CH_2$), 1.74-1.77 (m, 3H, -CH), 3.30 (d, 6H, J=12.8 Hz, $-CH_2$) and 7.54 (1H, $NH^+CF_3SO_3^-$).

TEHA Tosylate: ^{1}H NMR (400 MHz, $CDCl_3$, ppm): δ =0.88 (t, 18H, J=7.4 Hz, $-CH_3$), 1.19-1.33 (m, 24H, $-CH_2$), 1.71-1.74 (m, 3H, -CH), 2.34 (s, 3H, $-Ar-CH_3$), 2.65 (d, 6H, J=7.2 Hz, $-CH_2$), 7.15 (2H, d, J=3.9 Hz, Ar-H), 7.73 (2H, d, J=4.1 Hz, Ar-H) and 9.34 (1H, NH^+tosylate$^-$).

Techniques

The synthesized PILs have been confirmed by ^{1}H-NMR spectroscopy ASCEND^{TM}400 (Bruker, USA) relative to Tetramethylsilane (TMS). The melting temperature and the heat of fusion of the PILs were determined using a Q20 differential scanning calorimeter (TA Instrument, USA) in the range from -100 to 70 °C. The samples were heated at a scan rate of 5 °C/min under a nitrogen atmosphere.

Thermogravimetric analysis was performed on a TGA 4000 thermogravimetric analyzer (Perkin-Elmer, USA) under atmospheric conditions. Samples between 5 and 15 mg were heated from 20 to 650 °C under a constant heating rate of 20 °C/min. The sample chamber had a controllable environment to allow monitoring of the degradation under a dry nitrogen atmosphere. Experimental densities of PILs were measured by DDM 2910 (Rudolph Research Analytical, USA) in the temperature range of 20-90 °C. The apparatus is precise within 1.0×10^{-4} g.cm^{-3}, and the expanded uncertainty of the measurements was estimated to be better than 0.001 g.cm^{-3}. Calibration of the densitometer was performed at an atmospheric pressure using air dry and pure water (supplied). The refractive index was measured by RM40 refractometer (Mettler Toledo, USA). The measurement was taken at an atmospheric pressure and temperature range of between 20 and 90 °C, with a 10 °C increment. As for the viscosity study, the measurement was carried out using the Rheometer MCR301 (Anton Paar, Austria). The rheometer is a controlled stress (or controlled torque) instrument and was calibrated using standard viscosity oil. Temperature of the solution was maintained within ± 0.1 ºC. The viscosity was measured with an accuracy of less than 3 %. All measurements for each sample were performed in triplicate, and the values were reported as an average. The measurement was taken at an atmospheric pressure and temperature range of between 20 and 90 °C, with a 10 °C increment. Ionic conductivity was measured by the DZS-708 multi-parameter analyzer from Cheetah. This was carried out at an atmospheric pressure in temperatures ranging 25-70 °C with a 5 °C increment.

Table 2: Chemical Structure of Cations and Anions of Synthesized PILs Including the pK$_a$ of the Anions.

Cations		**Molecular Weight, g/mol**	**Charge delocalized by**	**pK$_a$**
Bis(2-ethylhexyl) ammonium	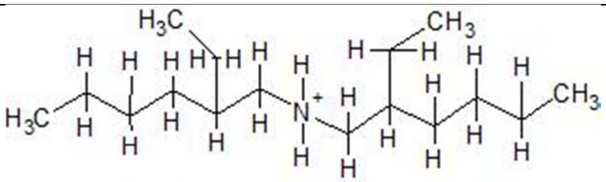	214		
Tris(2-ethylhexyl) ammonium	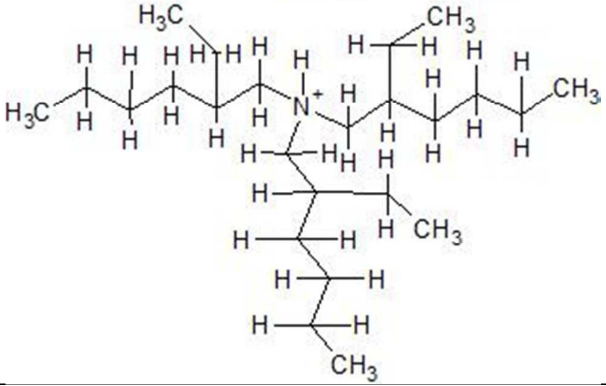	312		
Anions				
Trifluoroacetate		113	2 Oxygen atom	-0.25
Methanesulfonate	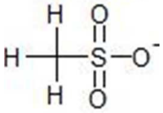	95	3 Oxygen atom	-2.6
Trifluoro methanesulfonate	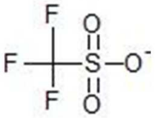	149	3 Oxygen atom	-14

Tosylate	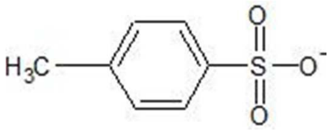	171	3 Oxygen atom	-2.8

Thermal conductivity measurement was carried out by the KD2 Pro (a product of Decagon devices, Inc.) in the temperature range of 20-70 °C, with a 10 °C increment at atmospheric pressure. This experiment was verified by measuring the thermal conductivity of water. The seebeck coefficient was obtained using the two beaker experiment method where two separate cells were connected through the salt bridge of the PIL/iodide redox couple solution. One of these two cells was heated and the other one was kept at room temperature. The Pt electrodes were used in cells and connected via a voltmeter (Agilent 34461A- 6½ Digit Multimeter). From the potential difference between the two cells increased with temperature at a linear rate, S_e values were obtained. The same setup of the Seebeck coefficient was used for the thermoelectrochemical device measurements. Additionally, a resistor box was connected in a parallel position with the voltmeter. This is to measure the potential at a fixed temperature difference at known resistances to calculate the current and output power of the thermoelectrochemical cells through the Ohm's law ($I = V/R$) and Joule's law ($P = I^2R = V^2/R$).

Results and Discussions

Thermal Stability

The decomposition temperature (T_d) is an important property for thermoelectric material as it reflects the thermal stability of the materials. Therefore, a high decomposition temperature is desirable for PILs as it results in a high utilization temperature range. The secondary and tertiary ammonium cations increase the decomposition temperature by increasing the branched chain of PILs. The intermolecular interaction between anions and cations are also responsible for the decomposition temperature. A very strong intermolecular interaction increases the decomposition temperature due to strong electrostatic interaction between the cation and anion. Hence more energy is required to break the chemical bonds.[37]

The thermal stability of PILs have been evaluated by the thermogravimetric analysis (TGA), and the traces of curves have been represented in Figure 1. As a result, the decomposition temperatures have been tabulated in Table 3. The decomposition temperatures are at $T_{5\%\ onset}$ which means the onset of the thermal decomposition curves for the first 5% weight loss. Drab *et al.*, reported that the values at $T_{5\%\ onset}$ provides a more accurate decomposition temperature than the onset of decomposition temperature.[38]

As a result of TGA, the decomposition temperatures of PILs are varied from 197.8 to 302.5 °C. In both, the series BEHA and TEHA, the TFA anion doped PILs has the lowest decomposition temperature of 204.8 °C and 197.8 °C. On the other hand, the TFMS anion doped PILs has the highest decomposition temperatures at 256.2 °C and 302.5 °C of PILs BEHA and TEHA series respectively. The thermal stability and the decomposition temperature can be correlated directly to the electrostatic force between the anion and cation.

In general, the dissociation constant of acid/anion is defined as the K_a values. The exponential numbers of dissociation constant was converted into a normal range by taking their negative logarithm, which is defined as pK_a, which represents the strength of acidity. The lower pK_a value is a stronger acidic in nature. The strong acid is able to form a strong chemical bonding with the cation. Hence it needs more energy to break the chemical bonding. Therefore, the stronger acidity of the anion exhibits a higher decomposition temperature. The pK_a values of all anions are listed in Table 2. Among these four anions, the TFMS has very low pK_a value (pK_a=-14) as a result of the decomposition temperature of TFMS containing PILs that is higher than the other members. On the other hand, the pK_a value of TFA (pK_a= -0.25) is higher than the other anions as, it is weakly acidic in nature. Hence, its decomposition temperature is lower than the other PILs. Given that all PILs have a decomposition temperature of 200-300 °C, this will be possible for use in energy harvesting from low grade energy sources.

PILs	M_w (g/mol)	T_d (˚C)	T_m (˚C)	H_f (J/g)	C_p (J/g.K)
BEHA TFA	327	204.8	49.2	70.4	11
BEHA MS	309	250.0	-11.2	23.66	0.827
BEHA TFMS	363	256.2	10.8	32.75	3.68
BEHA Tosylate	385	215.4	24.9	14.37	0.952
TEHA TFA	425	197.8	-70.8	3.01	0.418
TEHA MS	407	202.4	-62.8	6.11	0.422
TEHA TFMS	461	302.5	-69.9	3.51	0.293
TEHA Tosylate	483	228.3	-58.8	0.89	0.094

Table 3: Thermal Properties of the Synthesized PILs[†].

[†] M_w, T_d, T_m, H_f and C_p are molecular weight, decomposition temperature, melting temperature, heat of fusion and heat capacity respectively

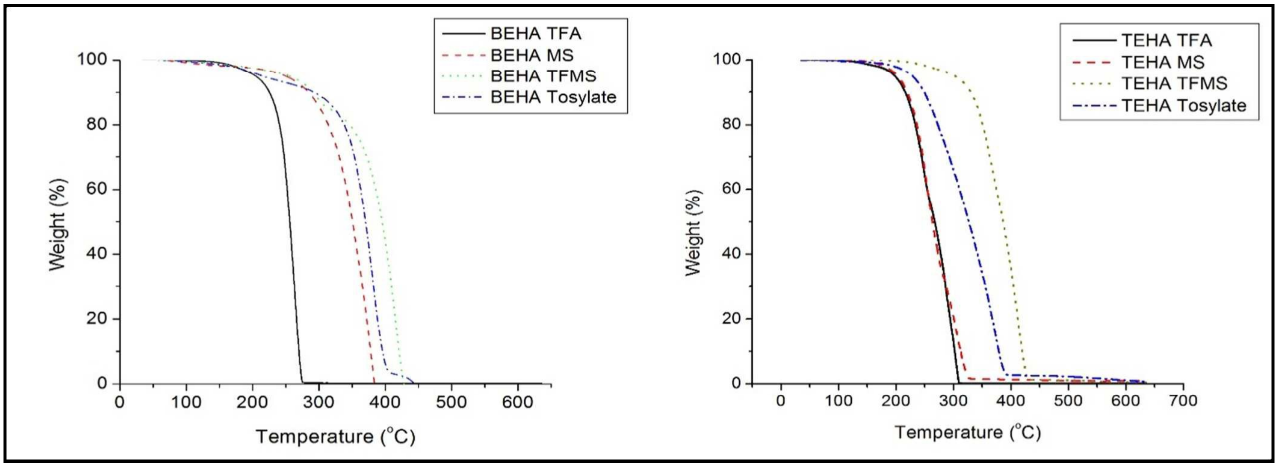

Figure 1 Characteristic Decomposition Curves of PILs (a) BEHA Series and (b) TEHA Series.

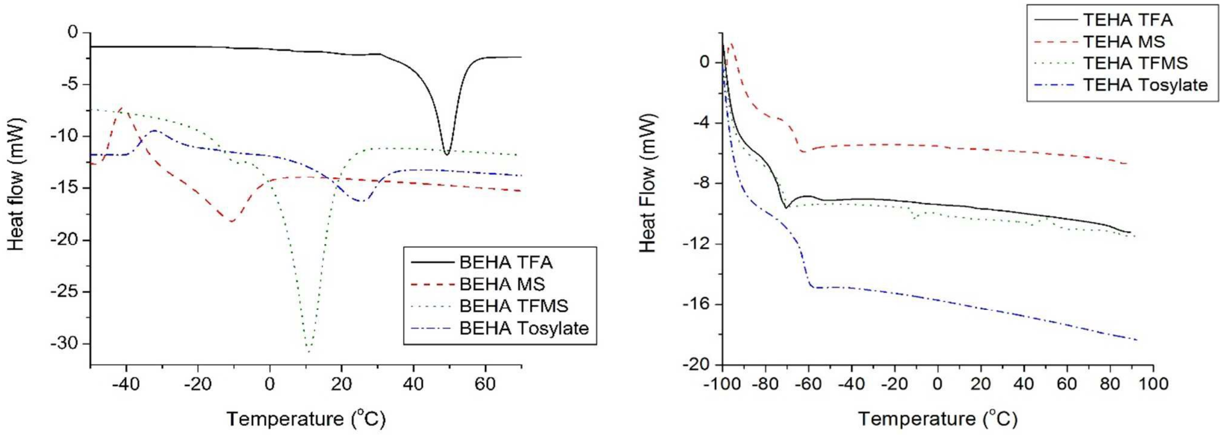

Figure 2 DSC Curves of the Synthesized PILs (a) BEHA Series and (b) TEHA Series.

Melting Temperature

The synthesized PILs listed in Table 1 have a broad range of melting points, from around -70.8 to 49.2 °C. In general, the melting point may be increased through increasing the packing efficiency of the ions. Several factors influence the melting points of the PILs which have been discussed in previous literatures[31, 38-43] including steric hindrance, packing efficiency, hydrogen bonding, interactions between anions and cations etc. The key factors are mainly the steric hindrance which disrupts the packing efficiency and minimize the hydrogen bonding of molecules.

In PILs of the BHEA series, among the 4 anions doped, the MS anion doped PILs shows a very low melting point (-11.2 °C) whereas all the remaining PILs show higher melting temperatures. BEHA MS contains the methyl sulphonyl group which gives more flexibility for PILs. The remaining anions TFA and TFMS contains highly electronegative fluorine atom which has the capability to form hydrogen bonding with the cationic hydrogen (from the secondary amine) atom more strongly. Hence, the BEHA TFA and BEHA TFMS possess higher melting temperatures of 49.2 °C and 10.8 °C respectively. The aromatic group containing BEHA Tosylate is highly rigid compared to the other members of this series hence it has a higher melting temperature (24.9 °C) than the BEHA MS and BEHA TFMS.

However, in the case of the TEHA series, the TEHA TFMS has a lower melting point (-69.9 ^{o}C) than TEHA MS (-62.8 ^{o}C) due to the interaction between anions and cations. Fluorine is more electronegative, thus contributes a greater number of hydrogen bonds. In comparing between the TEHA TFA (-70.8 ^{o}C) and the TEHA TFMS (-69.9 ^{o}C), the presence of the methyl sulfonyl group which gives a higher electronegative effect, is more favourable for hydrogen bonds, resulting in a higher melting temperature.

However, the aryl ring in TEHA the Tosylate provided a higher molecular weight (483 g/mol), which causes a higher melting temperature (-58.8 ºC).

In a comparison study of the BEHA and TEHA series, the anions of BEHA contribute to a very high melting temperature than the TEHA series. This may be due to the steric hindrance of the alkyl group, which is higher for the tertiary ammonium (TEHA) than the secondary ammonium (BEHA). Hence, this affects the molecular close packing of PILs of the TEHA series. Melting temperature is an inherent property of materials, and a low melting temperature is a required criterion for PIL. Therefore, low melting temperature is desirable, but it does not have a direct effect on the thermoelectric performance of PILs. From the DSC thermogram, the BEHA and TEHA series do not show glass transition temperature (T_g) in between our experimental temperature of -100 °C to 100 °C.

Heat of Fusion

Heat of fusion (H_f) is a specific amount of heat which is required to convert one gram of a solid to liquid state at its melting point without changing the temperature. This energy basically breaks down the solid bond, meanwhile leaving a significant amount of energy for the association of the intermolecular forces in the liquid state. Hence, a lower H_f is desirable for thermoelectric as it requires lower energy.

Heat of fusion is calculated by the peak area at melting temperature from the DSC curve. Thus, the sharper the peak, the greater the heat of fusion of the analysed compound.

$$Hf = {}^{Q}/_{m}$$

The values of heat of fusion of the synthesized PILs have been given in Table 3 which are obtained from the DSC curve. Heat of fusion depends on various factors such as functional groups, alkyl chain length, hydrogen bonds (within cation and interaction with anions), steric hindrance effect, electronegativity effect of the anions, cation volumes, molecular weight, and interaction force between anion and cations.[44, 45]

The clear endothermic peaks are observed in the DSC thermogram for the BEHA series which provides the information of heat of fusion. Among the four PILs of the BEHA series, the TFA anion doped PIL has the highest heat of fusion (70.4 J/g). The next candidate in this series is the TFMS anion doped PIL which possesses the heat of fusion of 32.75 J/g. Both electronegative fluorine substituted PILs (BEHA TFA and BEHA TFMS) have higher values, as fluorine increases the binding energy of the PILs. Hence, it requires higher energy to overcome the binding energy. The BEHA MS possesses the heat of fusion of 23.66 J/g[44, 45]. The lowest value, 14.37 J/g was obtained for the tosylate doped PILs (BEHA Tosylate). On the other hand, when a similar cation such as the TEHA is used, it shows different results from the BEHA group due to the anion-cation interactions between the TEHA cation and TFA, MS, TFMS and tosylate anions.[45]

In the presence of the similar anions like TFA, MS, TFMS and tosylate, the BEHA group has a higher heat of fusion value compared to the TEHA group due to the stearic hindrance effect. For example, the BEHA TFA has a value of 70.4 J/g H_f which is higher than TEHA TFA (3.01 J/g). Second degree amine of BEHA resulting in less hydrogen bonding leads to higher energy.[45]

Heat Capacity

Heat capacity is the required heat to increase 1 K temperature of 1 g substance. In other words, it can also be defined as the stored energy per molecule before the temperature increases. The heat capacity is calculated by the ratio of heat of fusion and the temperature difference of the melting peak. The unit is J/g.K. The calculated values of C_p from the DSC curve have been given in Table 3.

$$Cp = \frac{Q}{m\,\Delta T} = {}^{Hf}/_{\Delta T}\,\frac{J}{g.K}$$

The heat capacity values of the BEHA series are in the range of 0.827 to 11 J/g.K and the TEHA series are in the range of 0.094 to 0.422 J/g.K, and the mechanism of the thermoelectrochemical cells is to produce energy from the difference of temperature between the hot side and the cold side as it creates a temperature gradient. Therefore, the increment of temperature is deeply related to the mechanism of thermoelectricity as it is required to increase the temperature of the hot side to increase the temperature gradient in thermo-electrochemical cells. Generally, materials with a smaller heat capacity, will require lower energy to increase the temperature of the material. From Table 2, it is clear that BEHA MS and BEHA Tosylate possess the lowest heat capacity at 0.827 J/g.K and 0.952 J/g.K respectively. It requires very minimum energy to increase the temperature for 1K. The next higher heat capacity holding member of the series is the BEHA TFMS (3.68 J/g.K) as it needs little excess energy to boost up every 1K temperature for thermoelectrochemical cells. The BEHA TFA has very high heat capacity (11 J/g.K) among the formulations presented. The anion containing fluorine atom has a higher heat capacity than the other members and presence of higher alkyl chain length in cations decreases the heat capacity as TEHA has lower heat capacity than BEHA series.

Thermal Conductivity

The thermal conductivity results of the PILs at 20 and 70 ºC are tabulated in Table 4 and plotted in Figure 3 as a function of temperature in the range of 20 and 70 ºC, where it follows the normal trend of increasing with the increase of temperature.

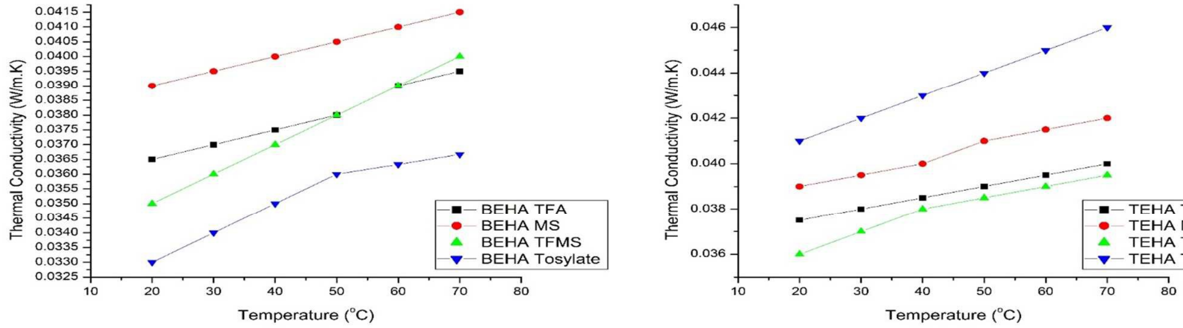

Figure 3 Thermal Conductivity of the Synthesized PILs in Combination with 0.05M I^-/I^{3-} at Various Temperature (a) BEHA Series and (b) TEHA Series.

Table 4: Density and Viscosity of Synthesized PILs and Ionic and Thermal Conductivity of the Fixed Ratio of PILs and 0.05M I^-/I_3^-

Temperature (˚C)	BEHA TFA	BEHA MS	BEHA TFMS	BEHA Tosylate	TEHA TFA	TEHA MS	TEHA TFMS	TEHA Tosylate
Thermal Conductivity, κ (W/m.K)								
20	0.0365	0.039	0.035	0.033	0.0375	0.039	0.036	0.041
70	0.0395	0.0415	0.04	0.03667	0.04	0.042	0.0395	0.046
Density, *ρ* (g/cm3)								
20	--	0.9806	1.0635	0.9995	0.9553	0.9387	1.0164	0.9648
90	0.9351	0.9330	1.0101	0.9523	0.9000	0.8914	0.9676	0.9193
Viscosity, *η* (Pa.s)								
20	--	1.07	0.622	1.74	0.357	2.41	1.72	4.3584
90	0.0109	0.032	0.0241	0.0435	0.0124	0.0498	0.0483	0.0944
Ionic Conductivity, σ (mS/cm)								
25	1.444	1.22	2.45	0.753	2.27	0.837	1.382	0.667
70	2.34	2.26	4.93	1.627	3.85	1.635	2.9	1.388

It is also noted that the effect of temperature is very negligible in some of the PILs.

The figure of merit ZT decreases with high thermal conductivity at any ΔT. Therefore, a lower thermal conductivity is desired for thermoelectrochemical cells where it increases ΔT and could be maintained across the device. The higher amount of alkyl chain length in cations increases the thermal conductivity as thermal conductivity depends strongly on the IL cation alkyl chain length. This is due to the dimensions of the IL bulk nanostructure being controlled by the cation alkyl chain consisting of the charged (ordered domains) and the uncharged regions (disordered domains). As the dimensions of the disordered domains are controlled by the cation alkyl chain, it limits the thermal conductivity.[46] From all the values of the thermal conductivity at various temperatures of the PILs, it is also noticeable that the thermal conductivity is not strongly dependent on the IL anion.[46] Additionally, another point is noticed which is the presence of fluorine and sulfonyl functional group in anions decrease the thermal conductivity. Despite this, the presence of benzene also increases the thermal conductivity. If the above points are considered, then it can be said that the fluorination of anions and lower amount of alkyl chain length are desirable criterion for the lower thermal conductivity as well as for the higher ionic conductivity.

In the presence of I^-/I^{3-} redox couple, the studied PILs demonstrate thermal conductivity in the range of between 0.033 to 0.041 W/m.K at 20ºC which is significantly lower than water (0.67 W/m.K), MPN (0.12 W/m.K), $[C_2mim][NTF_2]$ (0.12 W/m.K), $[C_2mim][B(CN)_4]$ (0.19 W/m.K).[5] From this discussion, it could be easily said that the PILs are very good candidates for thermoelectric materials with respect to its' thermal conductivity.

Density

Density values of the synthesized PILs at 20 and 90 ˚C temperatures are tabulated in Table 4. The findings indicate that the BEHA and TEHA series demonstrate temperature dependent behaviour, where the density decreases linearly with temperature increment as shown in Figure 4. Density of the synthesized PILs were affected by the packing of ions, size and shape of ions and interactions between ions.[47] Density decreases as the alkyl chain length increases in cations,[48, 49] which is the reason behind the higher density of BEHA than TEHA. In both series, the TFMS anion containing PILs has a higher density value which may be due to its high molecular weight of anions and two functional groups (fluorine and sulfonate) in the structure.[47] The decreasing trends of density has been observed while decreasing the molecular weight of anions except TFMS.

Viscosity

Since the operation of a thermoelectrochemical cell is done by mass transfer of the solution/ions from the hot to the cold side, the viscosity of the solution is critical. Ionic conductivity is directly affected by viscosity, the ionic conductivity decreases with the increase of viscosity.[7] Viscosity depends on the ion-ion interactions which mainly involve hydrogen bonding and van der Waals interactions.[48] Viscosity of ILs increase with the increment of alkyl chain length as it will provide stronger van der Waals interactions.[50] It is desirable to have low viscosities and high ionic conductivities for thermoelectric applications. The viscosity of the synthesized PILs at 20 and 90 °C are tabulated in Table 4.

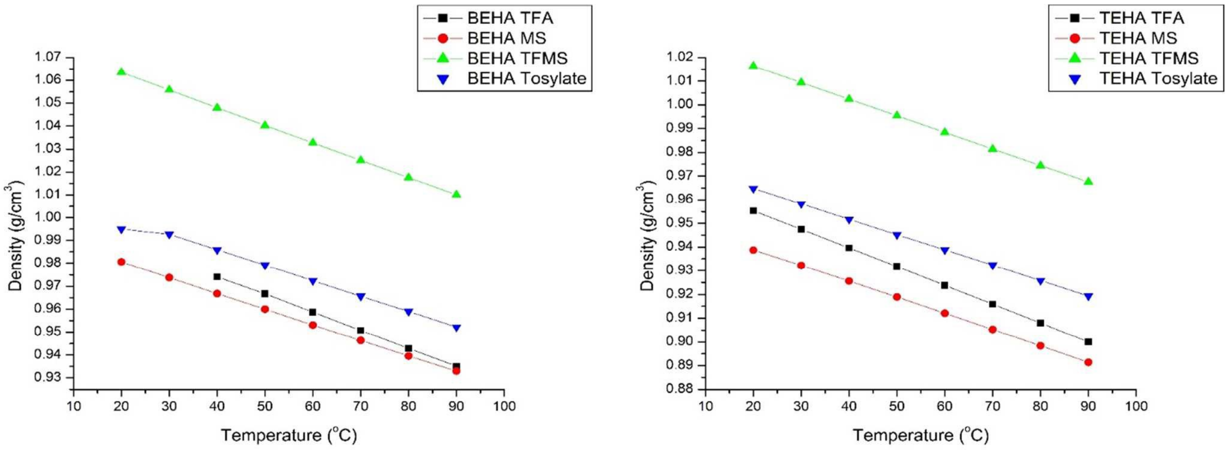

Figure 4 Densities of the Synthesized PILs at Different Temperature (a) BEHA Series and (b) TEHA Series.

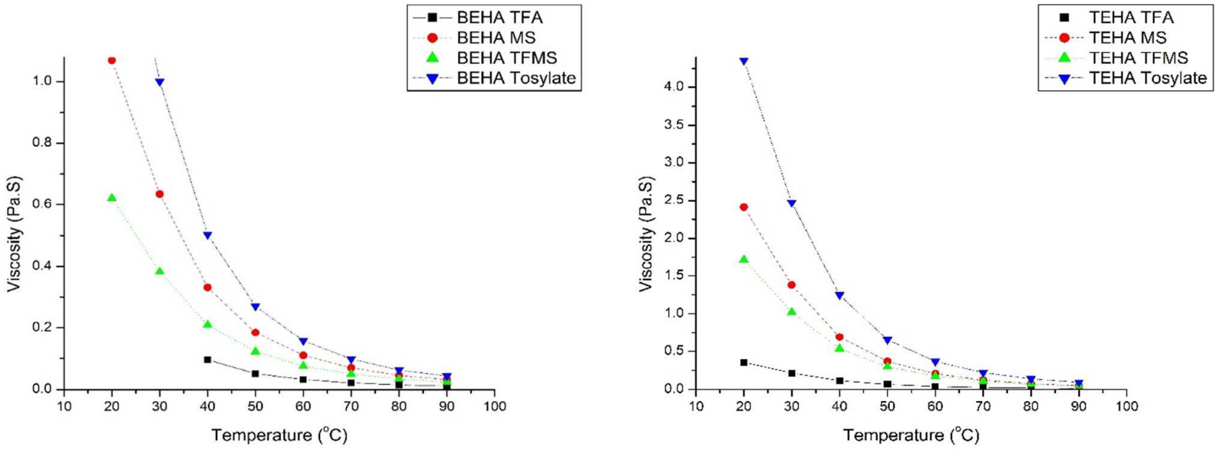

Figure 5 Viscosities of the Synthesized PILs at Different Temperature (a) BEHA Series and (b) TEHA Series.

Figure 5 shows the viscosity of the BEHA and TEHA series. For the BEHA series, the decreasing order of viscosity follows the trend as BEHA Tosylate> BEHA MS > BEHA TFMS > BEHA TFA decrease with the increase of temperature. A step decrease was observed while increasing the temperature from 20 °C to 50 °C. With further increase of temperature, the viscosity of PILs was not affected. In this series, the starting temperature of the BEHA TFA was observed from 50 °C because of its solid nature. Interestingly, BEHA TFA has low viscosity and which is not affected by temperature. It maintains a stable viscosity regardless of temperature. In the TEHA series, the decreasing order of viscosity of PILs is as follows: TEHA Tosylate> TEHA MS > TEHA TFMS > TEHA TFA. In both series, the same trend was observed with the decreasing viscosity with respect to the anion dopant in the PILs. Furthermore, all members constantly decrease the viscosity with respect to the temperature until 50 °C (except TEHA TFA). On further increase of temperature, it maintains the stable viscosity until 90 °C.

As noted from the BEHA series, TFA doped PIL possesses the unique property, where its viscosity is not affected by the temperature from 20 °C to 90 °C. Fluorine substituted anionic dopant containing PILs shows very low viscosity among the rest of the members. Amongst the fluorine substituted anions, the ionic size also plays a role, where the low molecular weight TFA has low viscosity than the higher molecular weight of TFMS. This concept is in good agreement with Ohno et al., report.[41]

Ionic Conductivity

Higher ionic conductivity is desirable for thermoelectric application as it increases the figure of merit ZT. The ionic conductivity at 25 and 70 ˚C are tabulated in Table 4 and are plotted in Figure 6 in the range of 25 to 70 ˚C where it is confirmed that the ionic conductivity increases with temperature as the normal trend.[7]

Amongst all the PILs, the PILs containing the fluorine atom in the anions, have the higher ionic conductivity as fluorine is more electronegative than hydrogen. The sulfonyl functional group in anions also help the PILs to have higher ionic conductivity than the acetate functional group. The presence of the benzene ring in anions decreases the ionic conductivity remarkably which is not a positive sign. On the other hand, a higher number of alkyl chain length in cations decreases the ionic conductivity. Therefore, it can be concluded that fluorination of the anions and lower alkyl chain length in cations are highly desirable in PILs for thermoelectrochemical applications.

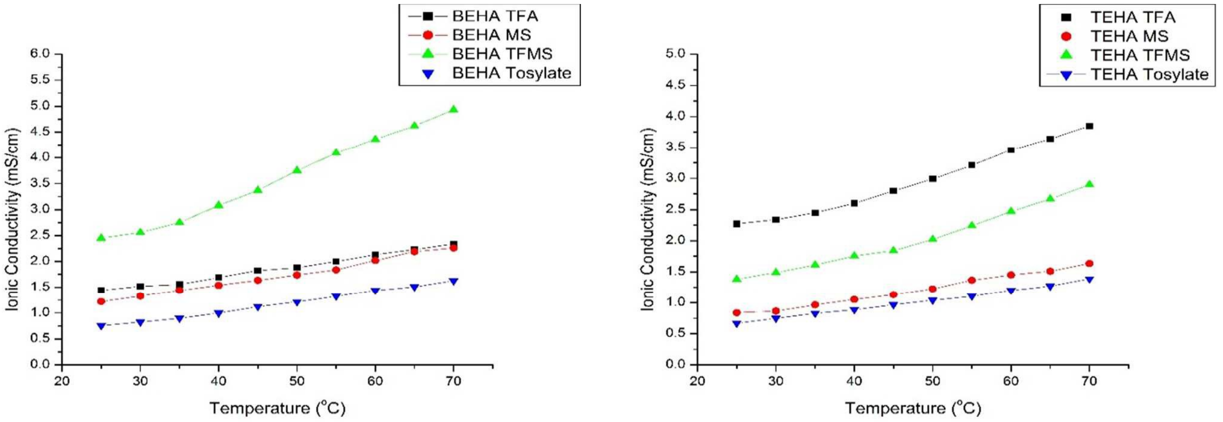

Figure 6 Ionic Conductivity of the Synthesized PILs in Combination with 0.05M I^-/I_3^- at Various Temperature (a) BEHA Series and (b) TEHA Series.

Table 5: Seebeck Coefficient, the Maximum Potentials (V_{max}), the Maximum ZT Values (ZT_{max}) Obtained using a Fixed Ratio of PILs and DMSO and 0.05 M I/I_3^-

PILs	Seebeck Coefficient (µV/K)	V_{max} (mV)	ZT_{max} ($\times 10^{-6}$)
BEHA TFA	340	11.68	758.04
BEHA MS	410	14.27	432.86
BEHA TFMS	370	14.89	949.46
BEHA Tosylate	376	15.18	253.65
TEHA TFA	182	7.03	281.23
TEHA MS	337	13.5	281.66
TEHA TFMS	420	14.92	548.68
TEHA Tosylate	352	14.55	192.79

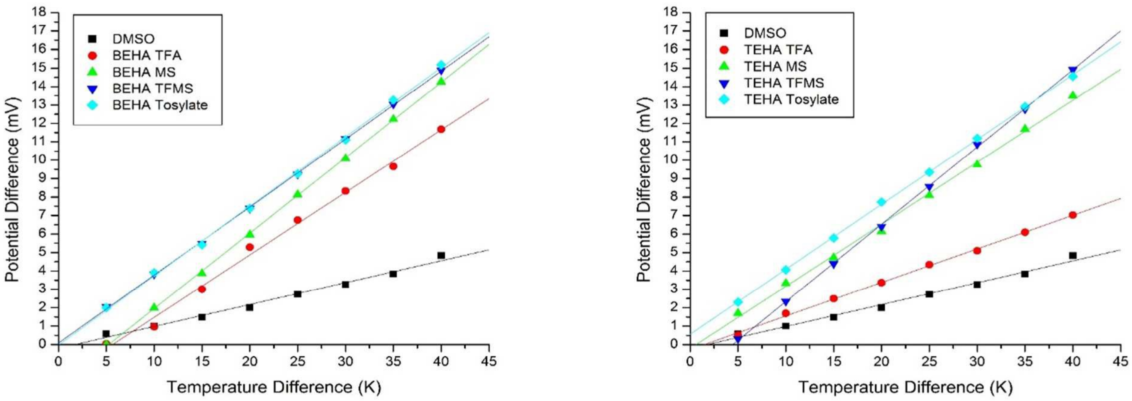

Figure 7 Seebeck Coefficient Measurements of the Synthesized PILs in Combination with 0.05M I-/I3- (a) BEHA Series and (b) TEHA Series

The PILs of our study with 0.05M I^-/I^{3-} redox couple have ionic conductivity in the range of 0.66 to 2.45 mS/cm at 25 ˚C and 1.38 to 4.95 mS/cm at 70 ˚C, which is higher than the AILs [HMIM][I], [PMIM][I], [BMPY][BF_4] reported by Stefanie et al.[7] where the ionic conductivities are 0.2, 1.6, 2.4 mS/cm at 25 ˚C respectively. Therefore, PILs could be a good candidate for thermoelectrochemical cells.

Seebeck Coefficient

The Seebeck coefficient and the maximum voltage of the PILs of this study with the combination of 0.05M I^-/I_3^- redox couple solution has been tabulated in Table 5 and the Seebeck coefficients were calculated from the Figure 7. The maximum voltage (V_{max}) for the PILs are in the range of 7.0 to 15.2 mV. The S_e values are 1.5 to 4 times greater when the solvents are PILs (182 to 420µV/K) than DMSO (119µV/K), which is a positive indication for the PILs as thermoelectric materials.

This Seebeck coefficient is directly related to the reaction entropy of the redox couple which is responsible for creating the potential difference across the thermoelectrochemical cells in the presence of the temperature gradient. The relation is as follows:

$$\partial E(T)/\partial T = S_e = \Delta S^o_{rc}/nF$$

where E(T) is the equilibrium electrode potential, which is a function of the temperature. T, S_e is the Seebeck coefficient, n is the number of electrons involved in reaction and F is Faraday's constant.[9, 51-56]

In comparison with the commonly used solid-state material Bi_2Te_3, which have S_e -287 µV/K, all the PILs of this study have a higher S_e (between 337 to 420 µV/K) except TEHA TFA (182 µV/K). All eight PILs with 0.05M I^-/I_3^- solution also have higher S_e values than the AILs [C_2mim][BF_4] (260 µV/K), [$P_{4,4,4,6}$][NTf_2] (170 µV/K), [C_2mim][NTf_2] (154 µV/K), [C_4mpyr][NTf_2] (60 µV/K), [C_2mim][B$(CN)_4$] (94 µV/K), [$P_{2,2,2,(101)}$][NTf_2] (30 µV/K) with 0.4M I^-/I_3^- solution, published by Abraham et. al., even it contains higher concentration of I^-/I_3^- redox couple as the S_e of the AILs increase with the concentration of I^-/I_3^- as the reported work[3] and also higher than [EMIM][CF_3SO_3] (364 µV/K), [HMIM][I] (-130 µV/K), [PMIM][I] (-190 µV/K).[7] The TEHA TFMS has the maximum Seebeck coefficient (420 µV/K). It can be expected from the above discussion that PILs could be a good alternative formulation to thermoelectric materials.

Figure of Merit

The efficiency of a thermoelectric material depends on the figure of merit ZT.

$$ZT = \sigma S_e^2 T/\kappa$$

Where σ is the ionic conductivity (S/m), S_e is the Seebeck coefficient (V/K), T is the absolute temperature (K) and κ is the thermal conductivity (W/m.K).

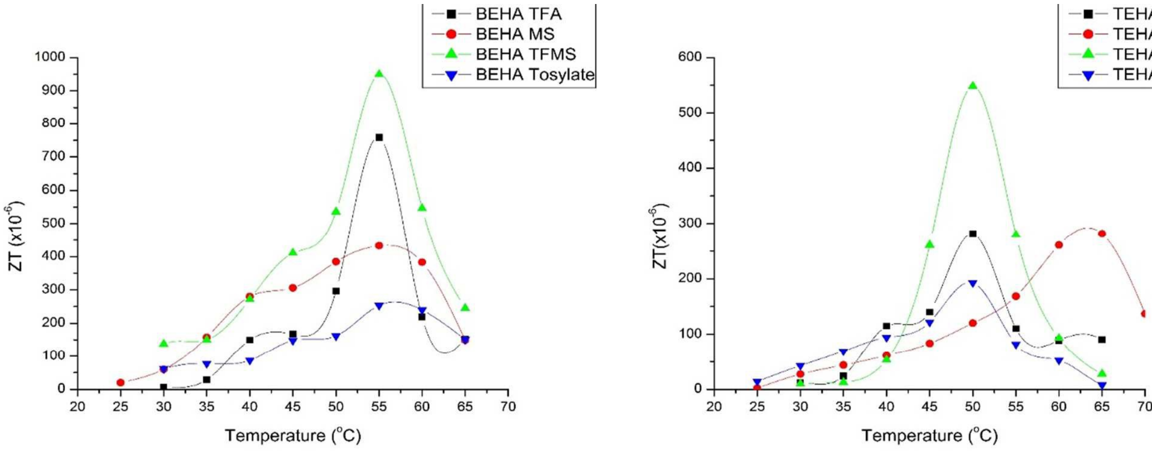

Figure 8 ZT of the Synthesized PILs in Combination with 0.05M I^-/I_3^- at Various Temperatures (a) BEHA Series and (b) TEHA Series.

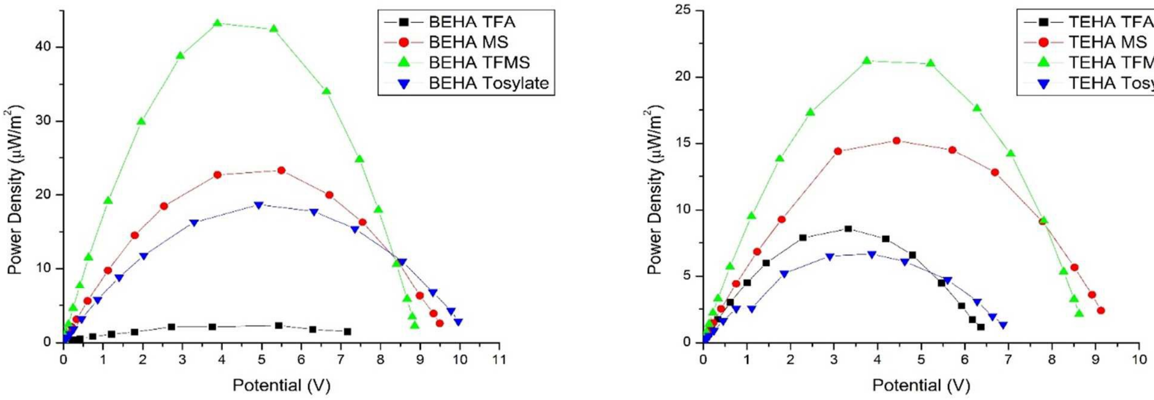

Figure 9 Thermoelectrochemical Cell Power Output Density Versus Potential Plots of the Synthesized PILs in Combination with 0.05M I^-/I_3^- at 25/50 °C (T_{cold}/T_{hot}) (a) BEHA Series and (b) TEHA Series.

The ZT values in the temperature range 30 to 65 °C of all the PILs are plotted in Figure 8 and the maximum ZT values are tabulated in Table 5.

From the above equation of ZT, it is clear that ZT is directly proportional to the ionic conductivity and Seebeck coefficient, as well as inversely proportional to thermal conductivity. Hence, the desirable properties are high ionic conductivity, high Seebeck coefficient and low thermal conductivity. PILs containing TFMS anions give the highest ZT values in both of the cases BEHA (949.46×10^{-6}) and TEHA (548.68×10^{-6}) as they have the lower thermal conductivity, higher ionic conductivity and higher Seebeck coefficient. On the other hand, Tosylate gives the lowest ZT values (BEHA 253.65×10^{-6} and TEHA 192.79×10^{-6}) as they have the higher thermal conductivity, lower ionic conductivity and lower Seebeck coefficient. The BEHA series normally gives the higher ZT values than the TEHA group as the thermal conductivity is higher, and the ionic conductivity and Seebeck coefficient are lower in the TEHA group than the BEHA group.

The maximum ZT values of our studied PILs are between $190x10^{-6}$ to $950x10^{-6}$ which are 1.5 to 46 times higher than some AILs like $[C_2mim][BF_4]$ ($130x10^{-6}$), $[C_2mim][NTf_2]$ ($39x10^{-6}$), $[C_4mpyr][NTf_2]$ ($33x10^{-6}$), $[C_2mim][B(CN)_4]$ ($28x10^{-6}$), $[C_2mim][DCA]$ ($21x10^{-6}$).[4] From these ZT values, the efficiency of PILs as thermoelectric materials can be easily understood and may be used for future thermoelectrochemical applications as electrolytes.

Power and Current output Density

The power and current output density was calculated from the measured potential values (V) and the known resistance (R) by the Ohm's law ($I = V/R$) and Joule's law ($P = I^2R = V^2/R$). The diameter of the Pt electrode is 1 mm. The maximum values of power and current output density are tabulated in Table 6.

Table 6: The Maximum Power Output Density (P_{max}) and Maximum Current Output Density (I_{max}) Obtained using a Fixed Ratio of PILs and DMSO and 0.05M I^-/I_3^-

PILs	T_{hot} (°C)/ T_{cold} (°C)	P_{max} (μW/m²)	I_{max} (mA/m²)
BEHA TFA	50/25	2.13	123
BEHA MS	50/25	23.3	75
BEHA TFMS	50/25	43.2	129
BEHA Tosylate	50/25	18.7	234
TEHA TFA	50/25	8.55	228
TEHA MS	50/25	15.2	531
TEHA TFMS	50/25	21.2	270
TEHA Tosylate	50/25	6.66	294

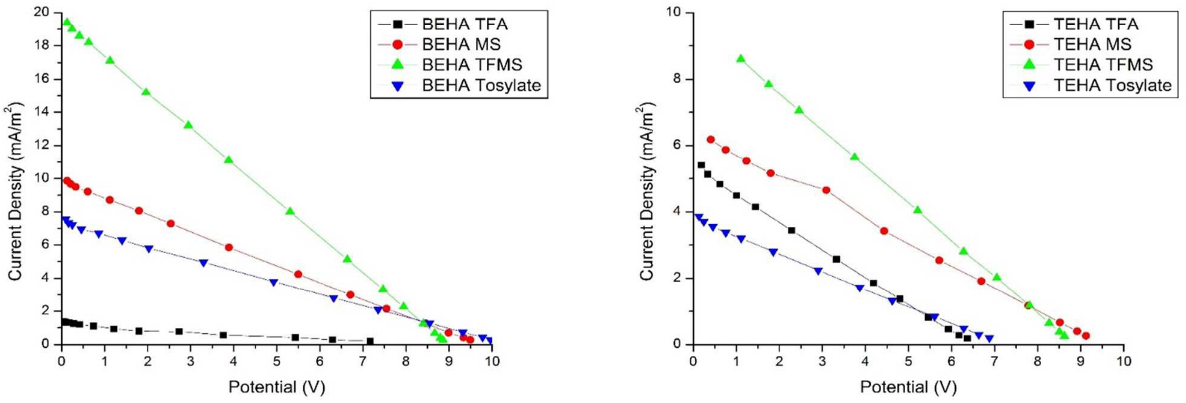

Figure 10 Thermoelectrochemical Cell Current Output Density Versus Potential Plots of the PILs in Combination with 0.05M I^-/I_3^- at 25/50 ºC (T_{cold}/T_{hot}) (a) BEHA Series and (b) TEHA Series.

The calculated values are plotted in Figure 9 and Figure 10 for power and current output density respectively and the trends of power and current output density with potential follows the same as previous literatures.[4-7] Abraham et. al reported 0.05 M $Fe(CN)_6^{3-}/Fe(CN)_6^{4-}$ in the [chaoline][DHP] PIL results in 0.1 mW/Kg power density when Pt was used as an electrode and it is independent of the solute-solvent ratio when the solvent is water.[6] Our aim of this study is to determine the eight different newly synthesized PILs' potentiality in thermoelectrochemical cells. Hence the experiments were carried out in a fixed solvent-solute ratio.

From the Ohm's and Joule's laws, it is noticeable that the current (I) is directly proportional to the potential (V) and power (P) is directly proportional to the current (I) as well as potential (V). Again, this current is directly related to the ionic conductivity as higher conductivity results in a higher current flow and lower conductivity results in lower current flow.

The maximum power density values of the studied PILs are from 2.13 to 43.2 µW/m^2. Between the BEHA and TEHA cations, BEHA has higher power output densities when the anions are the same, as the potential (V) (Table 5) is higher in the case of the BEHA group except for the BEHA TFA (2.13 µW/m^2) and TEHA TFA (8.55 µW/m^2). On the other hand, when the cations are same, TFMS has a higher power output than MS due to the higher output potential of TFMS, and with the TFA having a lower power output than the TFMS as TFA results in lowest potential. Hence, among all the PILs, the BEHA TFMS has the highest power density of 43.2 µW/m^2 as it results in an almost higher potential of 14.89 mV, and the BEHA TFA has the lowest power density of 2.13 µW/m^2 as it results in an almost lower potential of 11.68 mV.

The maximum current output density values of the studied PILs are in the range of 75 to 531 mA/m^2. When the cations are of similar BEHA, the TFMS has a greater current density than the TFA due to the higher ionic conductivity of BEHA TFMS (3.75 mS/cm) than BEHA TFA (1.879 mS/cm). The BEHA TFMS also has a higher ionic conductivity than BEHA MS (1.738 mS/cm), which results in the same order of current output density. On the other hand, the TEHA MS has a higher current density than the TEHA TFMS, which is not supported by their ionic conductivity as the ionic conductivity of the TEHA TFMS (2.02 mS/cm) is higher than the TEHA MS (1.226 mS/cm). TEHA MS has the greatest current density of 531 mA/m^2 and BEHA MS has the lowest current density 75mA/m^2.

The power and the current output of the studied PILs are higher than some of AILs such as [BMIM][BF_4], [EMIM][CF_3SO_3], [HMIM][I], [EAN][NO_3], [PMIM][I] and [BMPY][BF_4] which results in the range of 0.02 to 0.7 µW power output and 4 to 80 µA current output.[7] Hence, the PILs' performance as an electrolyte in the thermoelectrochemical device is also noticeable and could not be ignored.

Conclusion

The understanding of thermal and physical properties of the synthesized ammonium-based PILs is vital for its design and evaluation as thermoelectrochemical devices. Ammonium-based PILs have high potentiality for energy applications due to its basicity which leads to high ionic conductivity. Secondary and tertiary ammonium based two series (BEHA and TEHA) of PILs have been studied. The physical properties and stability with respect to the temperature of the PILs performed suitably to the thermoelectric materials. The BEHA series has the highest S_e values than the TEHA series. The maximum obtained S_e value is 420 µV/K, which is the highest reported in PILs in a I^-/I_3^- redox couple. As a result, the power and the current output of the studied PILs are higher, which shows that the PILs electrolyte coupled with the I^-/I_3^- redox couple is an attractive formulation for energy harvesting thermoelectrochemical generator.

Acknowledgement

The authors are grateful to the University of Malaya Centre of Ionic Liquids (UMCIL) for their assistance in the PILs synthesis and characterizations. This work has been financially supported by HIR (UM.C/625/1/HIR/MOHE/ENG/29), UMRG (RP006F-13SES), UMRG (RP023B-13AET), Science Fund (SF020-2013) and FRGS (FP011-A).

References

1. H. Kleinke, *Chemistry of materials*, 2009, **22**, 604-611.
2. J. Doherty, 2012.
3. T. J. Abraham, D. R. MacFarlane and J. M. Pringle, *Chemical Communications*, 2011, **47**, 6260-6262.
4. T. J. Abraham, D. R. MacFarlane, R. H. Baughman, L. Jin, N. Li and J. M. Pringle, *Electrochimica Acta*, 2013, **113**, 87-93.
5. T. J. Abraham, D. R. MacFarlane and J. M. Pringle, *Energy & Environmental Science*, 2013, **6**, 2639-2645.
6. T. J. Abraham, D. R. MacFarlane, R. H. Baughman, N. Li, Y. Chen and J. M. Pringle, 2013.
7. S. Uhl, E. Laux, T. Journot, L. Jeandupeux, J. Charmet and H. Keppner, *Journal of electronic materials*, 2014, **43**, 3758-3764.
8. D. R. MacFarlane, N. Tachikawa, M. Forsyth, J. M. Pringle, P. C. Howlett, G. D. Elliott, J. H. Davis, M. Watanabe, P. Simon and C. A. Angell, *Energy & Environmental Science*, 2014, **7**, 232-250.
9. T. Quickenden and Y. Mua, *Journal of The Electrochemical Society*, 1995, **142**, 3985-3994.
10. R. Hu, B. A. Cola, N. Haram, J. N. Barisci, S. Lee, S. Stoughton, G. Wallace, C. Too, M. Thomas and A. Gestos, *Nano letters*, 2010, **10**, 838-846.
11. N. M. Talavera-Prieto, A. G. Ferreira, P. N. Simões, P. J. Carvalho, S. Mattedi and J. A. Coutinho, *The Journal of Chemical Thermodynamics*, 2014, **68**, 221-234.
12. T. L. Greaves, A. Weerawardena, I. Krodkiewska and C. J. Drummond, *The Journal of Physical Chemistry B*, 2008, **112**, 896-905.
13. M. Hirao, H. Sugimoto and H. Ohno, *Journal of The Electrochemical Society*, 2000, **147**, 4168-4172.
14. P. Walden, *Bull. Acad. Imp. Sci. Saint-Pétersbourg*, 1914, 1800.
15. C. F. Poole, *Journal of Chromatography A*, 2004, **1037**, 49-82.
16. D. R. MacFarlane and K. R. Seddon, *Australian journal of chemistry*, 2007, **60**, 3-5.
17. K. Kurnia, C. Wilfred and T. Murugesan, *The Journal of Chemical Thermodynamics*, 2009, **41**, 517-521.
18. M. Iglesias, R. Gonzalez-Olmos, I. Cota and F. Medina, *Chemical Engineering Journal*, 2010, **162**, 802-808.
19. J. Sierra, E. Martí, A. Mengíbar, R. González-Olmos, M. Iglesias, R. Cruañas and M. Garau, 2008.
20. K. K. Laali and V. J. Gettwert, *The Journal of organic chemistry*, 2001, **66**, 35-40.
21. L. A. Blanchard, Z. Gu and J. F. Brennecke, *The Journal of Physical Chemistry B*, 2001, **105**, 2437-2444.
22. K. Fujita, D. R. MacFarlane and M. Forsyth, *Chem. Commun.*, 2005, 4804-4806.
23. X. Yuan, S. Zhang, J. Liu and X. Lu, *Fluid Phase Equilibria*, 2007, **257**, 195-200.
24. W. Tamura-Lis, L. Lis and P. Quinn, *Journal of Physical Chemistry*, 1987, **91**, 4625-4627.
25. M. A. Susan, A. Noda, S. Mitsushima and M. Watanabe, *Chemical Communications*, 2003, 938-939.
26. M. Picquet, I. Tkatchenko, I. Tommasi, P. Wasserscheid and J. Zimmermann, *Advanced Synthesis & Catalysis*, 2003, **345**, 959-962.
27. T. Jiang, H. Gao, B. Han, G. Zhao, Y. Chang, W. Wu, L. Gao and G. Yang, *Tetrahedron letters*, 2004, **45**, 2699-2701.
28. N. Bicak, *Journal of Molecular Liquids*, 2005, **116**, 15-18.
29. H.-M. Choi and I. Kwon, *Industrial & Engineering Chemistry Research*, 2010, **50**, 2452-2454.
30. M. J. Earle, N. V. Plechkova and K. R. Seddon, *Pure and Applied Chemistry*, 2009, **81**, 2045-2057.
31. U. Domanska and R. Bogel-Lukasik, *The Journal of Physical Chemistry B*, 2005, **109**, 12124-12132.
32. J.-P. Belieres and C. A. Angell, *The Journal of Physical Chemistry B*, 2007, **111**, 4926-4937.
33. M. Anouti, M. Caillon-Caravanier, C. Le Floch and D. Lemordant, *The Journal of Physical Chemistry B*, 2008, **112**, 9406-9411.
34. V. c. H. Álvarez, N. Dosil, R. Gonzalez-Cabaleiro, S. Mattedi, M. Martin-Pastor, M. Iglesias and J. M. Navaza, *Journal of Chemical & Engineering Data*, 2010, **55**, 625-632.
35. A. Pinkert, K. L. Ang, K. N. Marsh and S. Pang, *Physical Chemistry Chemical Physics*, 2011, **13**, 5136-5143.
36. M. Mahrova, M. Vilas, A. n. Domínguez, E. Gómez, N. Calvar and E. Tojo, *Journal of Chemical & Engineering Data*, 2012, **57**, 241-248.
37. T. Erdmenger, J. Vitz, F. Wiesbrock and U. S. Schubert, *Journal of Materials Chemistry*, 2008, **18**, 5267-5273.
38. D. M. Drab, M. Smiglak, J. L. Shamshina, S. P. Kelley, S. Schneider, T. W. Hawkins and R. D. Rogers, *New Journal of Chemistry*, 2011, **35**, 1701-1717.
39. M. Yoshizawa, W. Xu and C. A. Angell, *Journal of the American Chemical Society*, 2003, **125**, 15411-15419.
40. G.-h. Tao, L. He, N. Sun and Y. Kou, *Chemical communications*, 2005, 3562-3564.
41. H. Ohno and M. Yoshizawa, *Solid State Ionics*, 2002, **154**, 303-309.
42. H. Ohno, M. Yoshizawa and W. Ogihara, *Electrochimica Acta*, 2004, **50**, 255-261.
43. A. Bagno, C. Butts, C. Chiappe, F. D'Amico, J. C. Lord, D. Pieraccini and F. Rastrelli, *Organic & biomolecular chemistry*, 2005, **3**, 1624-1630.
44. Z. Zhang, A. A. Salih, M. Li and B. Yang, *Energy & Fuels*, 2014, **28**, 2802-2810.
45. E. A. P. Turner, C. C.; Singer, R. D., *Journal of Physical Chemistry A*, 2003, **107**, 2277–2288.
46. T. Murphy, L. M. Varela, G. B. Webber, G. G. Warr and R. Atkin, *The Journal of Physical Chemistry B*, 2014, **118**, 12017-12024.
47. T. L. Greaves and C. J. Drummond, *Chemical reviews*, 2008, **108**, 206-237.
48. Z. B. Zhou, H. Matsumoto and K. Tatsumi, *Chemistry-A European Journal*, 2005, **11**, 752-766.
49. Z.-B. Zhou, H. Matsumoto and K. Tatsumi, *Chemistry Letters*, 2004, **33**, 1636-1637.
50. 摇Bonhote, *Inorganic Chemistry*, 1996, **35**, 1168-1178.
51. J. Agar and W. Breck, *Transactions of the Faraday Society*, 1957, **53**, 167-178.
52. T. Licht and N. Swendeman, *Journal of The Electrochemical Society*, 1959, **106**, 616-625.
53. E. L. Yee, R. J. Cave, K. L. Guyer, P. D. Tyma and M. J. Weaver, *Journal of the American Chemical Society*, 1979, **101**, 1131-1137.
54. T. Quickenden and C. Vernon, *Solar Energy*, 1986, **36**, 63-72.
55. T. Ikeshoji, *Bulletin of the Chemical Society of Japan*, 1987, **60**, 1505-1514.

56. R. Hu, B. Cola, N. Haram, J. Barisci, S. Lee, S. Stoughton, G. Wallace, C. Too, M. Thomas and A. Gestos, *Nano Lett*, 2010, **10**, 838-846.

Synthesis and Characterization of Protic Ionic Liquids as Thermoelectrochemical Materials

T. A. Siddique,[a] S. Balamurugan,[a] S. M. Said,[a,*] N. A. Sairi,[b] and W. M. D. W. Normazlan[b]

[a] *Electrical Engineering Department, Faculty of Engineering, University of Malaya, 50603 Kuala Lumpur, MALAYSIA.*
E-mail: smsaid@um.edu.my, tawsif.mme07@gmail.com

[b] *Chemistry Department, Faculty of Science, University of Malaya, 50603 Kuala Lumpur, MALAYSIA*

*Corresponding author: smsaid@um.edu.my

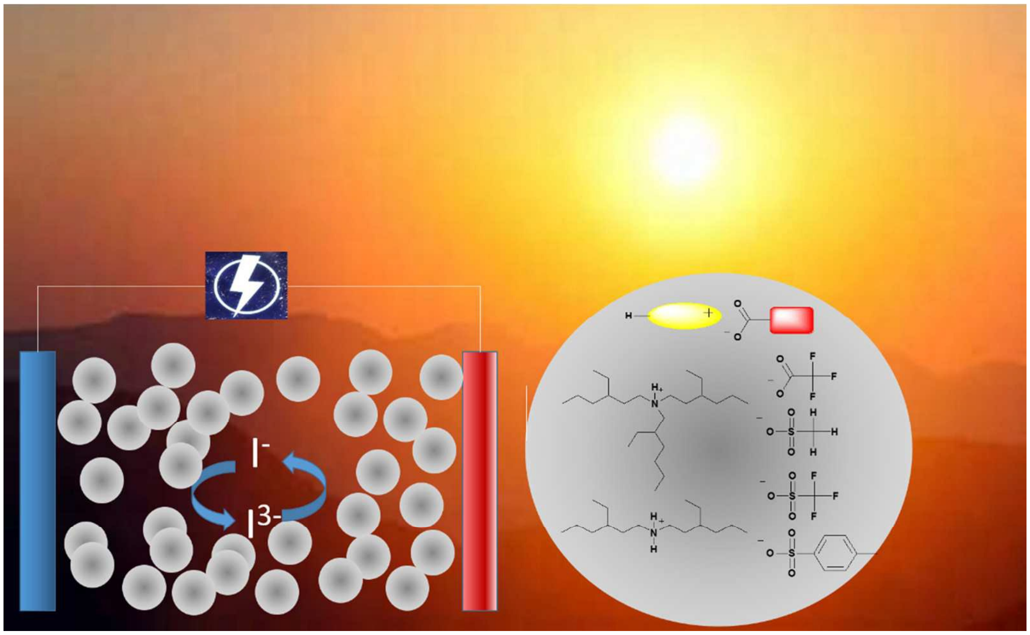

Highlights

PILs have been designed and synthesized for the energy harvesting applications. The module exhibited maximum S_e value is 420 μV/K which is the highest report in PILs of I^-/I_3^- redox couple.